

## **Rail vibrations: Data Analysis and FE Modelling with Applications to Signalling Equipment**

**A. Bracciali, M. Macherelli and F. Piccioli**  
**Dipartimento di Ingegneria Industriale**  
**Università di Firenze, Italy**

### **Abstract**

The paper shows the vertical vibration frequency response function of the rail on a sleeper, mid span and quarter span on a number of different tracks, highlighting the differences. Vibration data recorded during trains pass-by are compared, showing how the relevant railway standards may be misleading in some situations. A simplified finite element model of a track is developed to investigate the influence of railpad stiffness, poor tamping conditions and heavy masses connected to the rail. Heavy signalling equipment connected to the rail, e.g. an in-sleeper point machine, can significantly modify the rail vibration environment to which such equipment are subjected. General considerations are drawn on testing strategy both on line and in the laboratory to ensure both the best correspondence to real conditions and the feasibility of the test.

**Keywords:** rail, sleeper, vibrations, track, model, standard, point machine, signalling equipment.

### **1 Introduction**

Signalling equipment attached to rails and to sleepers are subjected to high stresses due to shock and vibrations. The authors dealt with the subject since many years [1][2] finding how the application of standards [3-7] is critical when the mass of the object considered is not negligible. A fundamental difficulty encountered when testing the heaviest objects of this category, i.e. an in-sleeper point machine, is that the acceleration spectra and the shock values requested by the standard cannot be obtained even with the biggest available shakers.

Track formation is an important factor to be investigated to understand its importance on the response of the rail/sleeper system to a given excitation and to

suggest possible design and testing strategies for signalling equipment depending on their application environment. As a general tendency, nowadays rails have a quite established profile (60 kg/m in Europe), railpads are relatively soft, concrete sleepers are considerably heavier than wooden sleepers (especially on high speed lines) and ballast and subgrades are carefully selected and maintained. There may be some relevant deviations from this scenario, for example in the case of slab track (where ballast is obviously missing and railpads are extremely soft in order to prevent shocks to damage the slab) or in turnouts where tamping is often poor due to intrinsic difficulties encountered with standard track tampers.

One of the most critical cases found is that of the in-sleeper point machine for the following reasons. First, for tolerance reasons the point machine is directly connected to the stock rails of the switch panel of the turnout; second, tamping conditions are rather poor and an abnormal dynamic settling of the rails can be observed during both low-speed and high-speed pass-bys; last but not least, modern point machines are modular and there is a number of components which may suffer from shock & vibrations especially when the track or the vehicle have some defects. Common situations are abnormal vibrations resulting from the poor geometry of the turnout insertion weld in the plain track and high shocks arising from wheel flats of defective rolling stock.

The paper aims at comparing the behaviour of a number both different and similar track formation in order to highlight any differences in the vertical dynamics which are the most relevant found in service. Then the spectra of vibrations encountered during revenue service in the same situations are analyzed, showing the differences with the spectra described in the standards. A simplified model of the vertical dynamics of a track is therefore shown where modifications are introduced, including the absence of railpad (direct fastening of the sleeper to the rail), an abnormal or absent stiffness of the sleeper support (“hanging sleeper”), and an extra mass loading. As aforementioned, all these conditions may be found in an in-sleeper point machine.

## **2 Available data**

The authors did vibration measurements during the last 15 years in several locations around Italy for different purposes. In some cases rail vibrations were measured during trains pass-by; in other cases (i.e. those campaigns devoted to the measurements of TDR – Track Decay Rate) rail vibrations were measured under a known excitation given by an instrumented hammer. Quite frequently both the sets were measured although not exhaustively, e.g. track response measurements were limited to a few points under known input instead of the whole set needed to estimate TDR.

Technology clearly evolved and acquisition details (DAQ boards, sampling frequency and frequency resolution) of the different campaigns are different but

nevertheless the data acquired in different conditions are sufficiently clear to perform a qualitative evaluation.

The analysis of the data will start from vertical point frequency response functions (FRF) measured in different locations (over a sleeper, quarter span and midspan) followed by the statistical analysis of rail and in-sleeper point machines vibrations during trains pass-by. Table 1 lists all the measurement campaigns conducted in the last 15 years, although not all of them are going to be used in the rest of the paper.

Year	Site (Italy)	Track	Type of Sleeper	Available Pass-by data	Available Point FRF		
					on sleeper	1/4 span	1/2 span
1998	Nozzano	B	CL	<i>Note 1</i>	✓	✓	✓
2000	Renacci	B	CH	✓	✓	✓	
2001	Incoronata	B	C	✓	✓	✓	✓
2004	Maccarese	B	ISPM	✓	<i>Note 2</i>		
2007	Lavino	B	C+ISPM	✓			✓ TDR
2010	Metronapoli	S	---				✓ TDR
2010	Fontanafredda	B	C	✓			✓ TDR
2011	Vaglia	B	CH				✓ TDR
2011	Renacci	B	CH				✓ TDR
2011	Rifredi	B	C				✓ TDR
2011	Ceprano	B	CH				✓ TDR
2012	Ozzano	B	Switch	✓			✓ TDR

Table 1: List of data available for track dynamic analysis

Note 1: not used as tested rolling stock was artificially made defective (wheel flats)

Note 2: not used as measurement done on the in-sleeper point machine

Key: B=ballast, S=slab, C=concrete, CH=concrete heavy, CL=concrete light, ISPM= in-sleeper point machine, Switch=switch panel.

### 3 Analysis of vertical point FRFs on the rail

Figure 1, Figure 2 and Figure 3 show the results of the analysis of point FRFs measured in different locations. The estimation of each FRF was made considering 5 impacts given by an instrumented hammer and the measurements were considered to be valid if the coherence function was consistently over 0.8.

The largest number of available FRFs is at midspan (Figure 1) as the TDR procedure, described in the relevant standard [8], requires the measurement in this location and in recent years the authors spent considerable time investigating the best conditions for this type of measurements that will be the object of a future paper. Only two point FRFs from the same campaign (Figure 2) were available at a quarter span and five FRFs from two campaigns were available over a sleeper

(Figure 3). This is linked to the fact that the former issue of prEN ISO 3095:2001 [9] required at those times such measurements. As this requirement disappeared in the version in 2005 [10], no measurements of such kind were subsequently performed. Also in this case the available data are nevertheless sufficient to draw some conclusions.

Although the data shown are in narrow band while a better comparison could be done in one-third octave band, the figures allow to conclude that while some features are quite evident in all the measurements, such as the “pinned-pinned frequency”, the actual amplitude of FRFs is quite erratic and hardly predictable in the whole frequency range. This is due to the intrinsic differences of the various tracks, namely those about rail constraints (railpads, clips, sleepers) and other local features that cannot be kept under control.

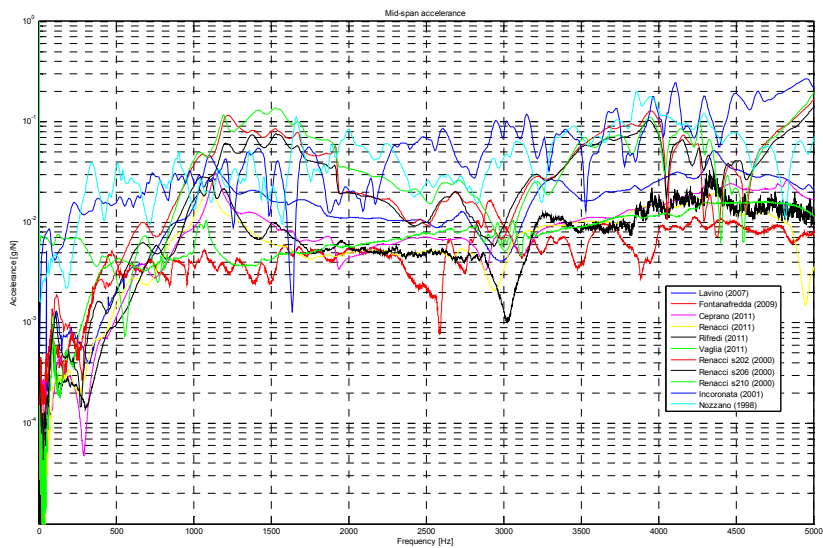


Figure 1: Vertical rail point FRF evaluated mid-span between two sleepers

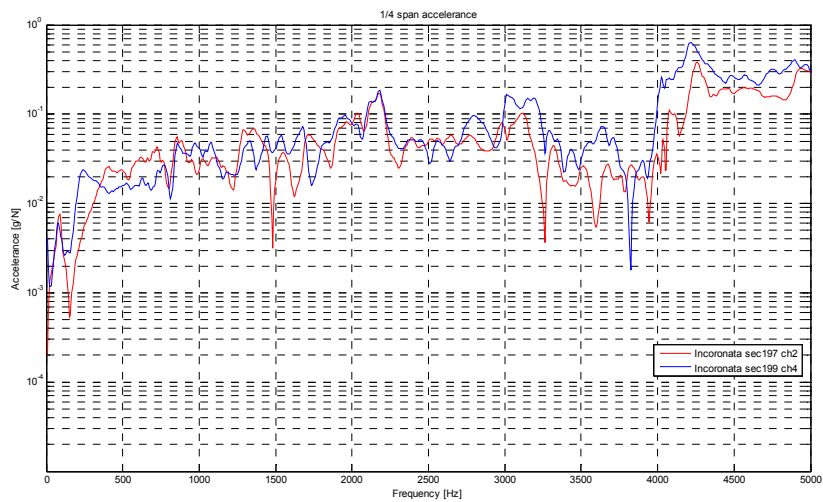


Figure 2: Vertical rail point FRF evaluated at 1/4 span between two sleepers

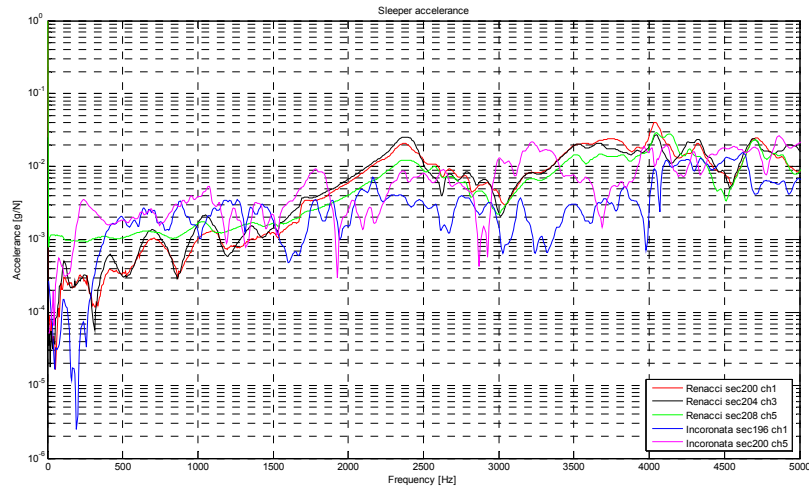


Figure 3: Vertical rail point FRF evaluated over a sleeper

This means that the same train running at the same speed in different locations can result in accelerations that may differ by a factor 10. Also the adoption of an average FRF is difficult because the average value may not be representative of any real track and also because a different average FRF should be considered along the rail, as it continuously changes.

## 4 Analysis of pass-by vertical rail accelerations

### 4.1 Introduction

In previous works the authors used sometimes the approach of “segmentation”, trying to extract the data from some portions of the time histories where bogies or wheelsets transit over the instrumented section. This aimed at trying to make the signals “as constant as possible” since statistical properties in terms of frequency content can better be found if the signal fulfils the classical requirements of signal processing [11]. Although this approach has its reasons, it was abandoned in this paper as:

- equipment connected to the rails and to the sleepers are subjected to rather high level of vibrations also away from the passing wheels, especially at the higher frequencies where the rail is particularly efficient as a waveguide and track decay rate is therefore low;
- train “segmentation” requires a quite complex processing that needs to know the “approximate” geometry of the train in terms of wheel arrangement, and this contrasts with the needs of an extensive reprocessing of the data from numerous and quite differently conducted measuring campaigns;
- working on levels ensures that no parts of the signal are neglected and that they are all properly accounted for and statistically considered.

The test campaigns analysed in this paper are shown in Table 2. It can be seen that a mixture of sleeper, midspan and quarter span is represented.

Test campaign	Renacci		Incoronata		Maccarese		Lavino		Fontanafredda		Mirandola	
Channels, position and section number (when applicable)	1	S 200	2	S 196	1	ISPM left	4	ISPM left	9	1/2 left	4	1/4 left
	2	1/2 202	4	1/2 198	2	ISPM right	7	ISPM right			5	1/4 right
	3	S 204	6	S 200								

Table 2: Vertical rail acceleration test campaign considered

## 4.2 Energy analysis and statistical considerations

A first data processing was done with the aim of calculating the energy levels (in terms of RMS values) along each train data and for each sensor. This was done by segmenting the data in frames of  $\Delta t=0.05$  s and calculating the corresponding acceleration  $a_{RMS}$  that was then classified in 0.5 g bins to evaluate its statistical distribution.

The  $\Delta t=0.05$  s time interval was selected as a compromise, giving a sufficiently high number of frames at the higher speeds (a passenger train with 12 vehicles running at 50 m/s (=180 km/h) results in around 150 frames) and a sufficiently low number of samples at the lower speeds (a 500 m freight train vehicles running at 25 m/s (=90 km/h) results in around 450 frames). The number of samples in the frame depends on the sampling frequency; as the latter was consistently around 10 kHz, it results in around 500 samples/frame, allowing the considerations described later about frequency distribution.

Figure shows as an example a passenger train measured in Ozzano (2012); time signals and  $a_{RMS}$  are shown. The number of samples is reduced by a factor 20 and the results are much less erratic than directly considering time histories.

All the trains from a measurement campaign can be therefore easily evaluated to give the corresponding distribution. As an example, all (160) the trains passed in Ozzano are shown in Figure 4. It is particularly interesting to see that there are several occurrences above the limits stated by [5] about the maximum total vertical acceleration (27 g) although this particular campaign lasted only 2 days. To evaluate the corresponding percentage of samples, the first two bins in the distribution (i.e. 0 and 0.5 g) were removed as they contain “quasi static” very low values which are numerous and bias the distribution.

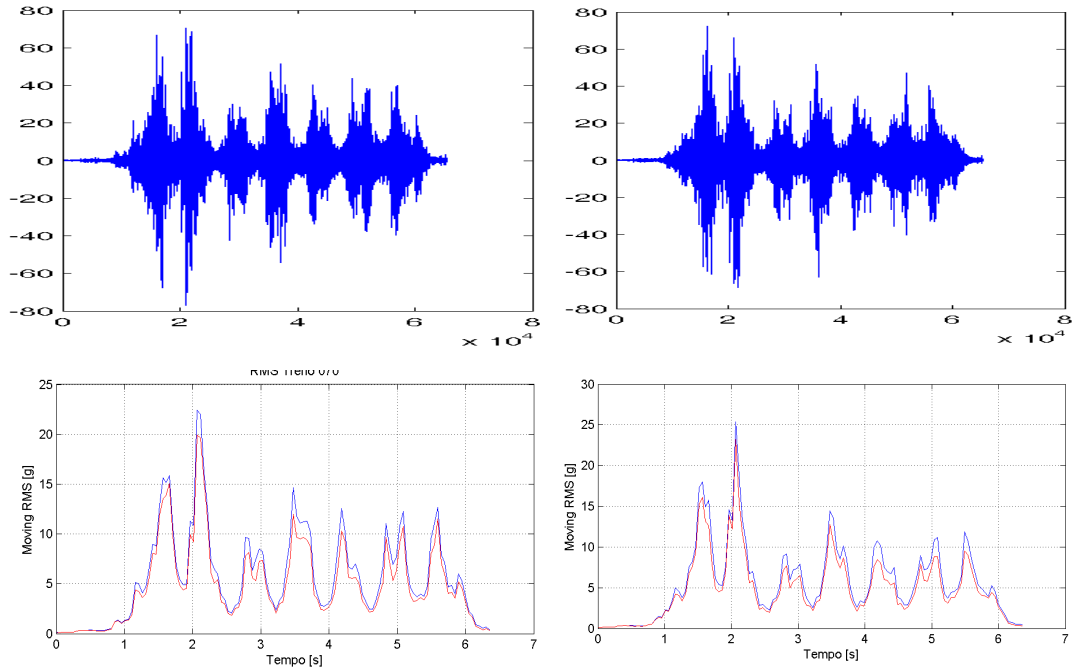


Figure 4: Time signal of the vertical acceleration of the two rails due to a passenger train running at 140 km/h (above) and  $a_{RMS}$  values calculated at time intervals of  $\Delta t=0.05$  s (below). Red plot is related to 2 kHz-low pass filtered signal while the blue plot is related to 5 kHz full-frequency signal analysis

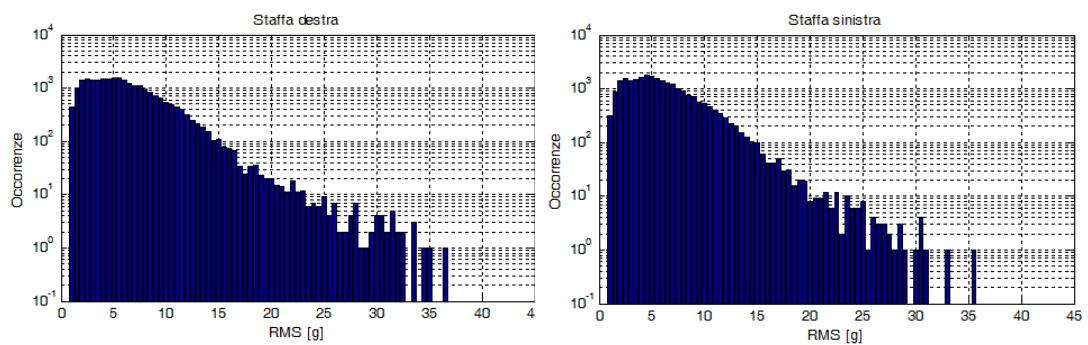


Figure 4. Distribution of  $a_{RMS}$  values for all the trains measured in Ozzano (2012).

The results for all sites cannot be reported here for reasons of space; Table 3 lists the number of frames that exceeded the threshold fixed by [5] considering the full data (5 kHz) or low-pass filtered data (2 kHz) according to the standard.

Site	Ch	$f \leq 2$ kHz			$f \leq 5$ kHz		
		No. samples	Samples > 27 g	%	No. samples	Samples > 27 g	%
Renacci	1	1325	0	0,00	2290	11	0,48
	2	2267	6	0,26	2557	16	0,63
	3	2177	0	0,00	2588	0	0,00
Incoronata	2	2538	13	0,51	2685	22	0,82
	4	2456	15	0,61	2644	23	0,87
	6	2295	2	0,09	2501	11	0,44
Maccarese	1	1857	0	0,00	2148	0	0,00
	2	745	0	0,00	1366	0	0,00
Lavino	4	16447	92	0,56	17365	129	0,74
	7	18220	127	0,70	18363	193	1,05
Fontanafredda	9	3840	21	0,55	3957	24	0,61
Ozzano	4	24944	7	0,03	25220	38	0,15
	5	25159	0	0,00	25394	12	0,05

Table 3: Frames considered in each measuring site with the number of frames for which the total spectral acceleration exceeded the limit of 27 g [5]

### 4.3 Frequency analysis and statistical considerations

Frequency analysis, i.e. the identification of the spectral properties of the recorded accelerations, was done by using the *perfect filtering* (also called FFT zero phase filtering) which consist in calculating the FFT of the entire signal and extract the frequency data by performing the inverse FFT (IFFT) only on the relevant portion of the spectrum. It has the advantage that statistical properties of the signal (for example the power spectrum) can therefore be computed also on very short frames as all the problems of digital (transient) and FFT (windowing) filter are intrinsically avoided. It has no ripple, infinite roll-off and cut-off frequencies coincident with band limits.

The aforementioned frames of  $\Delta t=0.05$  s can readily provide the spectrum when the definition of *power spectral density* (PSD) is applied to each of the frequency bands of interest. PSD can be computed from RMS by using the definition of the standard deviation and the PSD definition:  $PSD=RMS^2/\Delta f$ .

A statistical processing can be done on the set of PSD spectra obtained for each train; as an example Figure 5 shows the distribution of the spectra for the train seen above in the frequency range 0÷2000 Hz specified by [5] . In this specific case it can be seen that there is in practice no correspondence between the limit curve described in the standards and the spectra recorded on the rails. Although not shown here, also the frequency content above 2 kHz is significant but not considered by the standard.



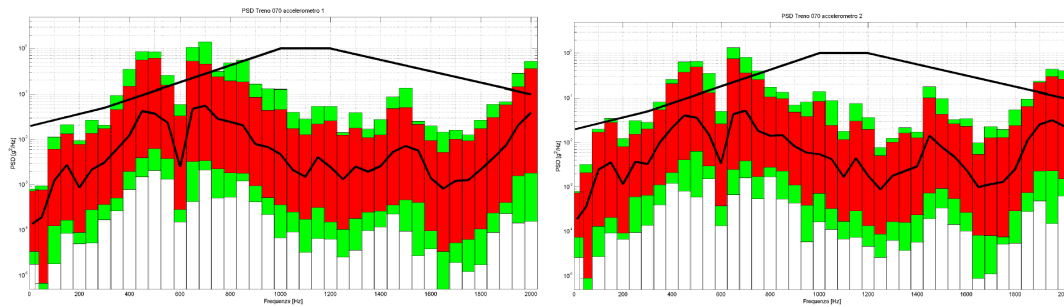


Figure 5: Spectra for all the frames for the train shown in Figure for both rails. Thick line is the 50 percentile (median) of all the spectra; red bars show the 5÷95 percentile interval and green bars show the 0.15÷98.5 percentile interval. Also shown is the limit described in [5]

Results for all the considered measuring campaigns are shown in the following figures represent PSD [g<sup>2</sup>/Hz] vs. frequency [Hz]. The 5V limit curve is plot as well. The following conclusions can be drawn:

- Renacci is situated on the high-speed line (250 km/h) Florence-Rome. Rails 60E1 are supported by heavy concrete sleepers (400 kg). Ballast tamping is optimal. All PSD curves are below the 5V limit [5] except for a small exceedence in channel 3 between 1600 and 2000 Hz. The energy is mostly concentrated at high frequency as train speed is quite high;
- Incoronata is situated on the conventional line (180 km/h) Foggia-Bari in the South of Italy. Rails 60E1 are supported by standard concrete sleepers (260 kg). Ballast tamping is standard. PSD curves are below the 5V limit, and one of the curves copies with the 98.5 percentile that limit. Low frequency anomalies should not be taken into account;
- Maccarese is situated on the conventional line (160 km/h) Grosseto-Rome. Measurements were taken on the connections between the rails and the in-sleeper point machining equipping the turnout 6B. Ballast tamping is very poor. PSD curves are well below the 5V limit and the shape of the median curve is quite different from the one described in the standard. This can be due to a combination of very poor tamping and heavy inertia due to the high mass of the in-sleeper point machine;
- Lavino is situated on the conventional line (200 km/h) Bologna-Milan equipped with 60E1 rails. Measurements were taken on the connections between the rails and the in-sleeper point machining equipping the turnout 7A. Ballast tamping is poor. Both channels exceed the 5V limit of the PSD. A bad insertion weld of the turnout and the relatively high speed (190 km/h) may be responsible for this. The 0.15 percentile curve is the fact the highest of all considered measuring campaigns
- Fontanafredda is situated on the conventional line (140 km/h) Treviso-Pordenone in the North-East of Italy. Measurements were taken on one point on the left 60E1 rail. Sleepers are of standard FS type. Ballast tamping is average. Data

dispersion is relevant and the overall shape of the 98.5 percentile almost copies the 5V limit curve;

- Ozzano is situated on the conventional line (140 km/h) Bologna-Rimini. Measurements were taken on the connections between the rails and the switch blade check equipment installed on turnout 3A. Ballast tamping is standard. PSD curves show a relevant exceedence of the 5V limit together with a “trough” at around 600 Hz and a trend much different from 5V limit.

Summarizing, some curves well fit the 5V limit but there are some important limitations (see Figure 12 showing the 50 and 98.5 percentiles of PSD):

1. the presence of poor tamping and/or heavy masses influence the response of the track to vertical excitations. In these cases the spectra are much lower and considering the standard 5V limit could lead to a serious overestimation of vibration loads during type testing;
2. the trend of the curve is often very different from the 5V limit curve, especially in the mid frequency range (where accelerations are lower) and in the low frequency range (where accelerations can be higher);
3. as long as the position on the rail, i.e. over a sleeper or at the midspan, heavily influences the rail response, a generic sentence such as “rail vibrations” should state where the component is going to be mounted on the rail.

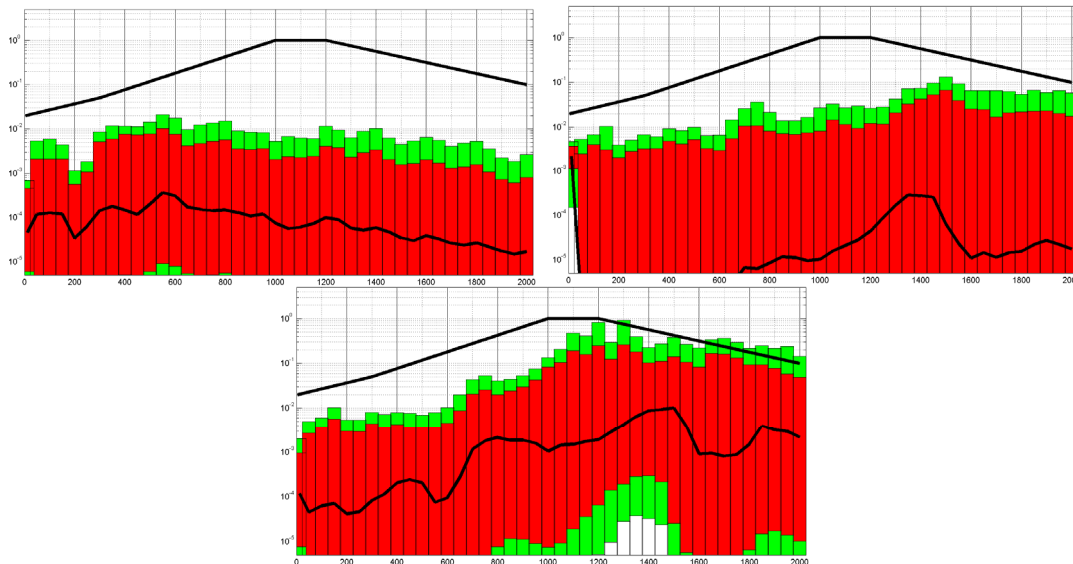


Figure 6: Spectra for sections 200 (on sleeper), 202 (midspan) and 204 (on sleeper) in Renacci for all measured trains.

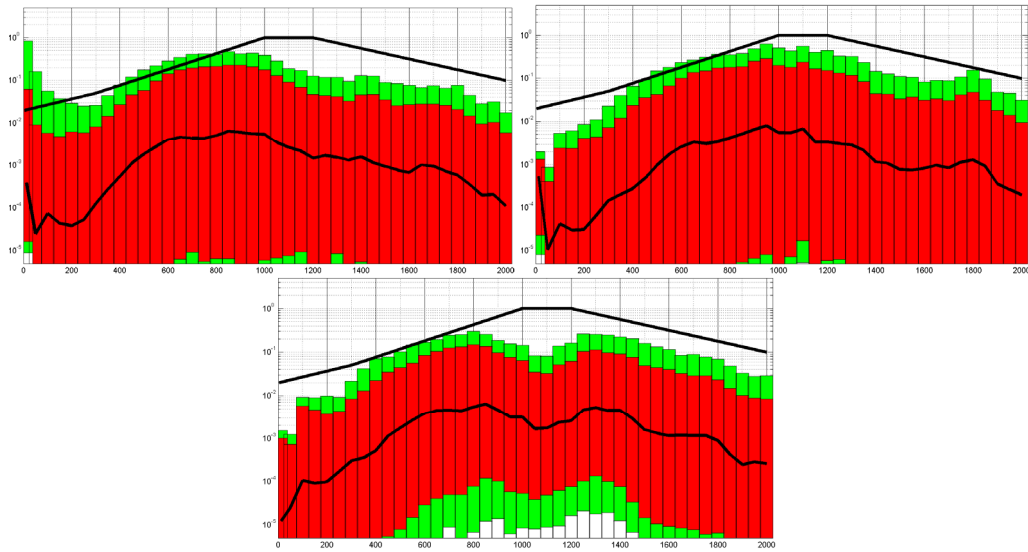


Figure 7: Spectra for sections 196 (on sleeper), 198 (midspan) and 200 (on sleeper) in Incoronata for all measured trains

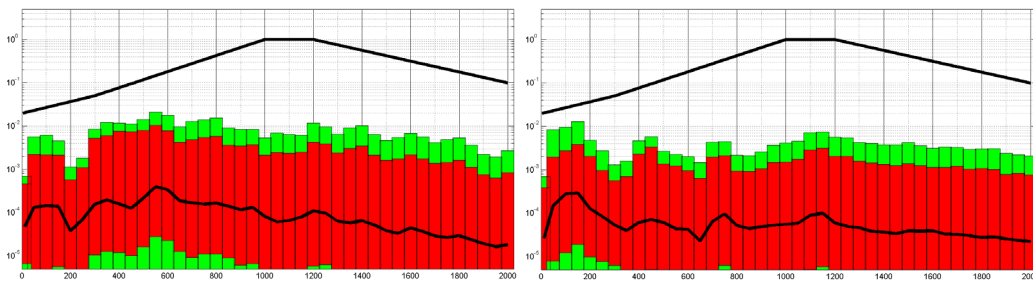


Figure 8: Spectra for left and right rail vibrations in Maccarese for all measured trains

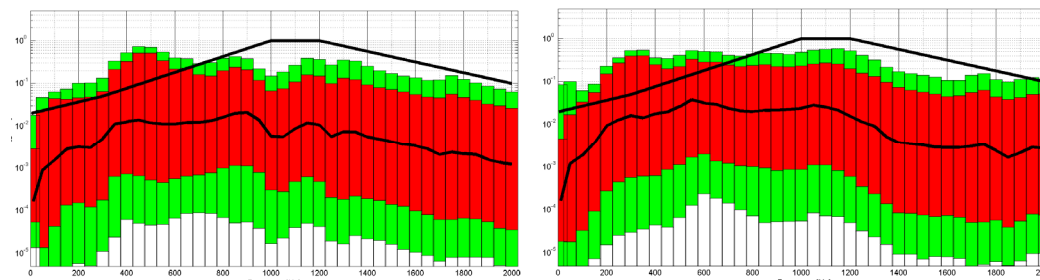


Figure 9: Spectra for left and right rail vibrations in Lavino for all measured trains

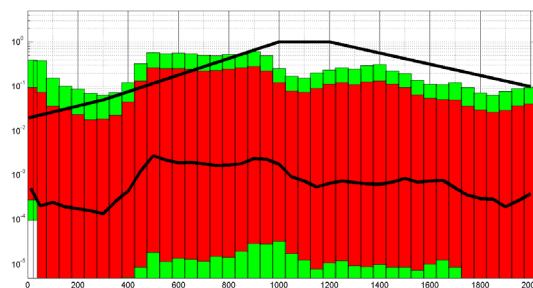


Figure 10: Spectra for left rail vibrations in Fontanafredda for all measured trains

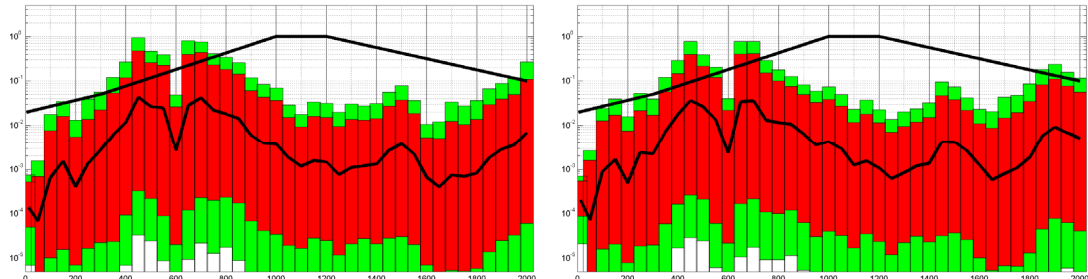


Figure 11: Spectra for left rail vibrations in Ozzano for all measured trains

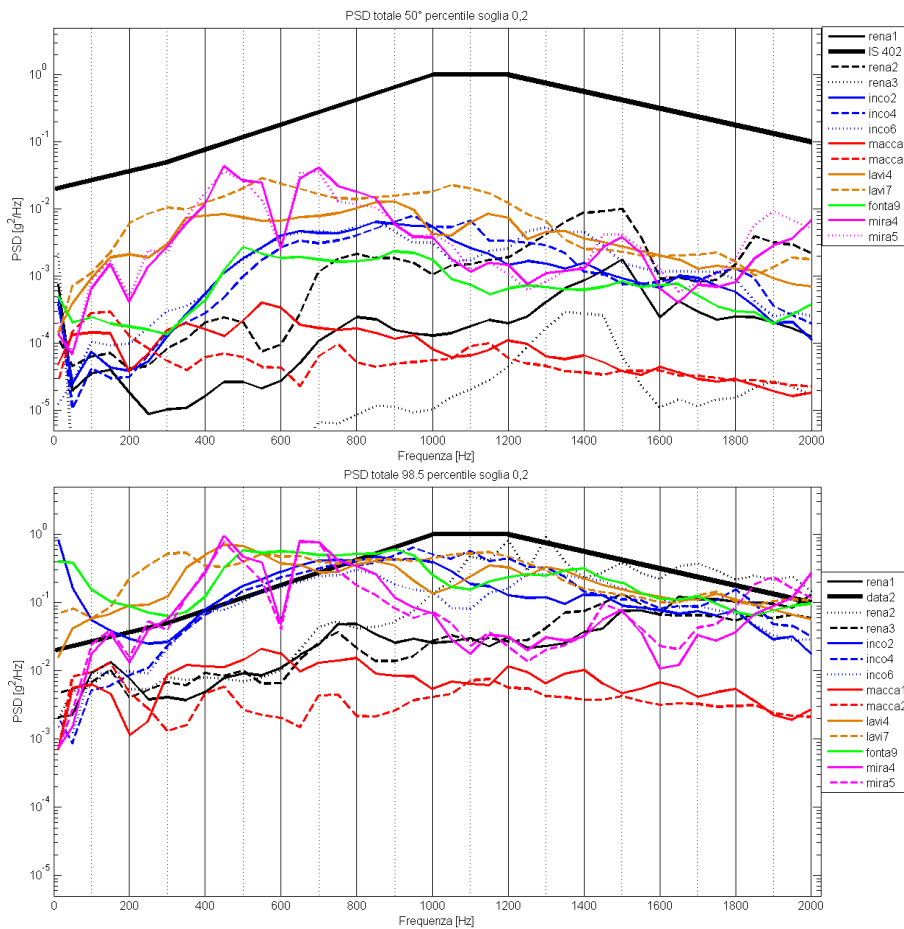


Figure 12: Fifty (top) and 98.5 (bottom) percentile PSD curves for all analysed campaigns

## 5 Evaluation of track modifications with a FE model

### 5.1 Introduction

Finite element modelling of the track is well developed and it was not the intention of the authors to either develop a particularly advanced model or to refine the existing models. A simple model based on a Timoshenko beam on discrete supports

of the vertical dynamics of a rail was developed with the unique goal of finding a reasonable justification of the behaviour observed in service.

A sketch of the model is shown in Figure 13. The FE model was built with the ANSYS software; the 60E1 rail is made of BEAM189 elements 2 mm long, while the sleeper is modelled through a MASS21 concentrated mass ( $m_s=220$  kg) and the rail fastening is modelled with a spring-damper COMBIN14 element ( $k_b=300$  kN/mm,  $c_b=80$  kNs/m) as the ballast ( $k_b=80$  kN/mm,  $c_b=57$  kNs/m) below each half-sleeper. As only one rail was considered, sleeper and ballast properties were appropriately halved. As the rail is infinite in nature, the model was built long enough to make the boundary effects negligible. Eighty sleeper spans were considered with a total length of 48 m (with the standard spacing of 0.6 m). The model is fully parametric.

Unitary harmonic loads from 10 to 2000 Hz were applied “on support” (i.e. over the sleeper) and “midspan”. Rail vibrations and sleeper vibrations were compared to check the degree of “isolation” given by the fastening that the sleeper gets benefit from and “reverse effect” of the different boundary conditions on rail vibrations under the same excitation. Responses in any other points can be taken but as the in-sleeper point machines are usually installed in place of a sleeper they will not be considered here.

The model was verified by comparison with the available literature, checking the quasi-static behaviour and the classical features returned by these models (pinned-pinned resonance, sleeper acting as tuned damper, etc.). No further details of the model tuning and check will be given here.

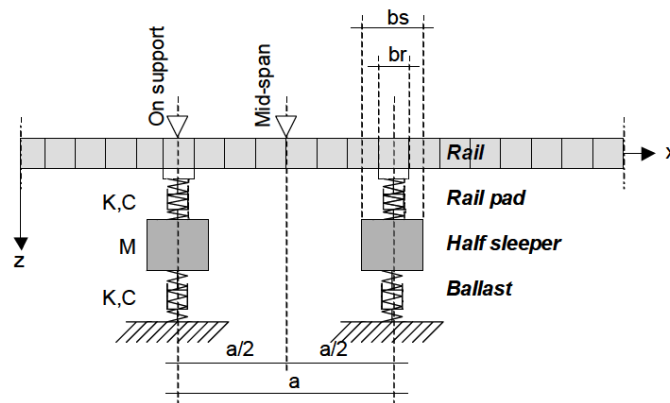


Figure 13: Model of the vertical dynamics of a rail to investigate the effect of poor tamping and of heavy objects attached to the rail.

## 5.2 Effect of sleeper mass

The response functions due to a heavier “sleeper” (representing the an in-sleeper point machine) with a mass  $m_s=800$  kg are shown in Figure 14 where the responses on both the rail and the sleeper underneath are compared to the standard case where

$m_s=220$  kg, considering the standard fastening system. As long as the response is measured “on support” the pinned-pinned resonance is seen as an antiresonance where the rail is “hinged”; clearly this frequency and the amplitude of rail response are not affected by the mass of the sleeper but the amplitude of the sleeper response at this frequency decreases proportionally to its mass (inertia), i.e. by a factor  $800/220=3.6$ . The benefit of increasing the mass of the sleeper is somewhat limited but, in any case, the response on rail is deeply modified at the lower frequencies (e.g. at 140 Hz the rail response is around 6.7 times lower with the heavier sleeper) where some minor advantaged can be obtained.

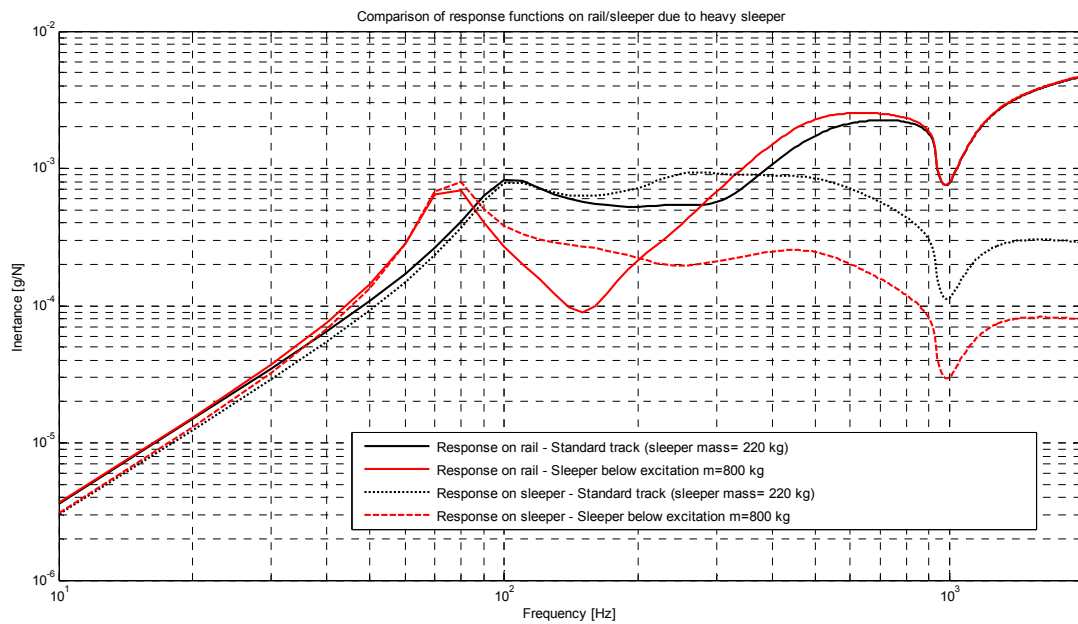


Figure 14: Effect of a heavy sleeper attached to the rail (standard fastening and tamping) on the frequency response function of the rail and the sleeper

### 5.3 Effect of railpad stiffness and bad tamping

A more complete evaluation can be done by looking at results shown in Figure 15. The response on rail and sleeper in standard conditions is shown again for comparison with the situation where there is no pad (i.e. it has an infinite stiffness, the usual mounting condition for in-sleeper point machines) and the tamping is bad under the considered support. It can first of all be seen that bad tamping has only a very limited effect at very low frequencies (well below 100 Hz) and that above 200 Hz the response of the rail/sleeper (which are rigidly connected in this case) is insensitive to tamping conditions. Effects on rail can then be observed, showing how the rigid fastening of the sleeper can reduce by a factor from 2 (for  $200 \text{ Hz} \leq f \leq 300 \text{ Hz}$ ) to around 10 (for  $f = 700 \text{ Hz}$ ) the vertical vibrations of the rail compared to the standard case.

It is evident that when a heavy mass is rigidly connected to the rail the response of rail changes dramatically and this justifies the different behaviour shown in Maccarese and, to a lower extent, in Ozzano. It is worth to remind that the results in Lavino are heavily affected by a bad weld and are therefore not fully reliable for the present analysis.

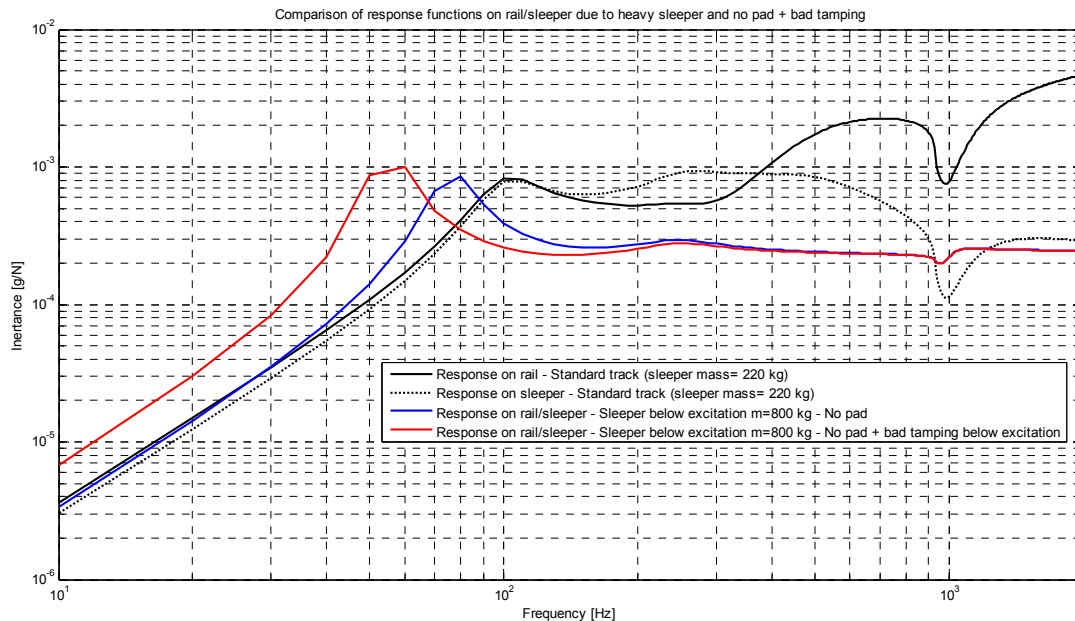


Figure 15: Effect of an infinitely rigid rail/sleeper fastening and of poor tamping on the frequency response function of the rail and the sleeper

## 6 Conclusions and further developments

The analysis (or re-analysis in most of the cases) of data coming from numerous test campaigns showed that rail vibrations remains a complex subject where standards appear to be barely sufficient in just a few cases.

Vertical track response to known loads was discussed showing how, beyond some key features that all the tracks exhibit, details vary heavily case by case making impossible to define a “standard” or “reference” track which fits all the possibilities that can be found in practice.

Statistical analysis of vibrations recorded during trains pass-by was done with a simple methodology. Compared to other analyses performed by the authors in the past, it is “blind” and can be easily applied to collect data during further activities as long as it requires only accelerometers. Vertical loads are those that are statistically applied to rails without any approximations.

Rail vertical vibrations spectral analysis showed distributions where exceedence of highest limits occurs a relevant number of times. In this case the international

standards on type testing look inadequate to describe what happens on the track during real service. Frequency analysis, performed with an original methodology, shows that testing signalling equipment on a shaker may result in completely wrong conclusions as the statistical distribution of energy along the frequency span may be significantly different from limit curves described in the standards.

To describe and justify some of the behaviours observed in real life, a simple finite element model of the vertical dynamics of the rail was built. Results are consistent to what is expected, i.e. the local application of heavy masses rigidly connected to the rail deeply affects rail vibrations, with reductions of even an order of magnitude. It can be concluded that in the case of an in-sleeper point machine a modified limit curve for type testing should be introduced after specific tests.

## References

- [1] A. Bracciali, A. Rossi: “Vibrazioni nelle apparecchiature di segnalamento ferroviario collegate al binario”, XXXIV convegno AIAS, Milano 2005 (in Italian).
- [2] A. Bracciali, F. Piccioli, L. Di Benedetto, “Vibrations in Signalling Equipment: Limitations and Improvements of Current Standards”, Proceedings of the Thirteenth International Conference on Civil, Structural and Environmental Engineering Computing, Crete, 6-9.9.2011 (on CD).
- [3] EN 50125-3, Railway applications - Environmental conditions for equipment. Part 3: Equipment for signalling and telecommunications, 2004.
- [4] ERRI A 118 Rp 4, European Rail Research Institute (ERRI): Use of electronic components in signalling – Non-electrical environment in the case of electronic signalling systems.
- [5] Rete Ferroviaria Italiana, Prove di Tipo e di Accettazione per le apparecchiature elettroniche ed elettromeccaniche destinate agli Impianti di Sicurezza e Segnalamento – Specifica Tecnica IS 402, 2000.
- [6] IEC 60068-2-64, Environmental testing - Part 2-64: Tests - Test Fh: Vibration, broadband random and guidance, 2008.
- [7] EN 60068-2-27, Environmental testing, Part 2-27: Tests - Test Ea and guidance: Shock, 2009.
- [8] EN 15461, Railway applications - Noise emission - Characterisation of the dynamic properties of track sections for pass by noise measurements, 2008.
- [9] prEN ISO 3095, Railway applications – Acoustics - Measurement of noise emitted by railbound vehicles, 2001.
- [10] EN ISO 3095, Railway applications - Acoustics - Measurement of noise emitted by railbound vehicles, 2005.
- [11] M. P. Norton, D. G. Karczub: Fundamentals of Noise and Vibration Analysis for Engineers, Cambridge University Press, 2003.